

19. P. König, A. K. Engel, W. Singer, *Trends Neurosci.* **19**, 130 (1996).
20. P. J. Clyne *et al.*, *Neuron* **22**, 327 (1999).
21. Q. Gao, B. Yuan, A. Chess, *Nature Neurosci.* **3**, 780 (2000).
22. L. B. Vosshall, A. M. Wong, R. Axel, *Cell* **102**, 147 (2000).
23. P. Mombaerts *et al.*, *Cell* **87**, 675 (1996).
24. G. Laurent, M. Naraghi, *J. Neurosci.* **14**, 2993 (1994).
25. Y.-W. Lam, L. Cohen, M. Wachowiak, M. Zochowski, *J. Neurosci.* **19**, 749 (1999).
26. K. MacLeod, A. Bäcker, G. Laurent, *Nature* **395**, 693 (1998).
27. M. Stopfer, S. Bhagavan, B. H. Smith, G. Laurent, *Nature* **390**, 70 (1997).
28. M. Wehr, G. Laurent, *Nature* **384**, 162 (1996).
29. K. MacLeod, G. Laurent, *Science* **274**, 976 (1996).
30. M. Heisenberg, A. Borst, S. Wagner, D. Byers, *J. Neurogenet.* **2**, 1 (1985).
31. J. Dubnau, L. Grady, T. Kitamoto, T. Tully, *Nature* **411**, 476 (2001).
32. S. E. McGuire, P. T. Le, R. L. Davis, *Science* **293**, 1330 (2001).
33. T. Zars, M. Fischer, R. Schulz, M. Heisenberg, *Science* **288**, 672 (2000).
34. F. C. Kenyon, *J. Comp. Neurol.* **6**, 133 (1896).
35. B. Leitch, G. Laurent, *J. Comp. Neurol.* **372**, 487 (1996).
36. G. Laurent, M. Wehr, H. Davidowitz, *J. Neurosci.* **16**, 3837 (1996).
37. Materials and methods are available as supporting material on Science Online.
38. Most KC spikes occurred in the beginning of the response: response intensity was 2.33 ± 2.02 spikes over the first 1.4 s; PNs produced 12.84 ± 7.29 spikes on average in that period.
39. Responses were determined here according to method A (37). Nearly identical results were obtained if responses were assessed by different criteria adapted to each population (figs. S4 and S5).
40. B. Willmore, D. J. Tolhurst, *Network Comput. Neural Syst.* **12**, 255 (2001).
41. B. S. Hansson, S. Anton, *Annu. Rev. Entomol.* **45**, 203 (2000).
42. Although we have not characterized this spikelet pharmacologically, its shape and all-or-none waveform suggest the involvement of voltage-dependent conductances (possibly Na^+ or Ca^{2+} for depolarization and K^+ for repolarization), consistent with previous patch-clamp studies in vitro (43).
43. S. Schafer, H. Rosenboom, R. Menzel, *J. Neurosci.* **14**, 4600 (1994).
44. PCT application to the MB did not affect the LFP oscillations recorded there, for the principal source of these oscillations—synchronized, periodic synaptic input drive from PNs—was excitatory and cholinergic (nicotinic).
45. D. Fricker, R. Miles, *Neuron* **28**, 559 (2000).
46. M. Galarreta, S. Hestrin, *Science* **292**, 2295 (2001).
47. F. Pouille, M. Scanziani, *Science* **293**, 1159 (2001).
48. D. Contreras, A. Destexhe, M. Steriade, *J. Neurophysiol.* **78**, 335 (1997).
49. L. B. Haberly, in *Cerebral Cortex*, E. G. Jones, A. Peters, Eds. (Plenum, New York, 1990), pp. 137–166.
50. Z. Zou, L. F. Horowitz, J.-P. Montmayeur, S. Snapper, L. B. Buck, *Nature* **414**, 173 (2001).
51. H. Barlow, *Ann. N.Y. Acad. Sci.* **156**, 872 (1969).
52. A. Livermore, D. G. Laing, *J. Exp. Psychol. Human Percept. Perform.* **22**, 267 (1996).
53. C. Linster, B. H. Smith, *Physiol. Behav.* **66**, 701 (1999).
54. W. S. Cain, B. C. Potts, *Chem. Senses* **21**, 35 (1996).
55. M. Abeles, H. Bergman, E. Margalit, E. Vaadia, *J. Neurophysiol.* **70**, 1629 (1993).
56. A. Riehle, S. Grün, M. Diesmann, A. Aertsen, *Science* **281**, 34 (1997).
57. P. Duchamp-Viret, B. Palouzier-Paulignan, A. Duchamp, *Neuroscience* **74**, 885 (1996).
58. T. Tanabe, M. Iino, S. F. Takagi, *J. Neurophysiol.* **30**, 1284 (1975).
59. J. W. Nemitz, S. J. Goldberg, *J. Neurophysiol.* **49**, 188 (1983).
60. Supported by the National Institute for Deafness and other Communication Disorders; the National Science Foundation; the McKnight, Alfred P. Sloan, and Keck Foundations (G.L.); a Sloan and Swartz Foundations fellowship (J.P.-O.); a Department of Defense

National Defense Science and Engineering graduate fellowship (O.M.); the Elizabeth Ross fellowship (G.C.T.); and a Helen Hay Whitney postdoctoral fellowship (R.L.W.). We thank M. Westman for his intracellular PN data; C. Pouzat for help with spike sorting; S. Farivar for help with the immunocytochemistry; the Laurent Lab; E. Schuman, A. Siapas, and C. Mead for discussions; M. Roukes for help with silicon tetrodes; I. Lubenov and A. Siapas for help with wire tetrodes; M. Walsh for electronics; and the Caltech Biological Imaging Center for their resources and expertise. Multichannel silicon probes were provided

by the University of Michigan Center for Neural Communication Technology sponsored by NIH NCRR grant no. P41-RR09754.

Supporting Online Material

www.sciencemag.org/cgi/content/full/297/5580/359/DC1

Materials and Methods

Figs. S1 to S5

Movie S1

4 February 2002; accepted 31 May 2002

Regulation of Cerebral Cortical Size by Control of Cell Cycle Exit in Neural Precursors

Anjen Chenn^{1,2*} and Christopher A. Walsh^{2†}

Transgenic mice expressing a stabilized β -catenin in neural precursors develop enlarged brains with increased cerebral cortical surface area and folds resembling sulci and gyri of higher mammals. Brains from transgenic animals have enlarged lateral ventricles lined with neuroepithelial precursor cells, reflecting an expansion of the precursor population. Compared with wild-type precursors, a greater proportion of transgenic precursors reenter the cell cycle after mitosis. These results show that β -catenin can function in the decision of precursors to proliferate or differentiate during mammalian neuronal development and suggest that β -catenin can regulate cerebral cortical size by controlling the generation of neural precursor cells.

A massive increase in the size of the cerebral cortex is thought to underlie the growth of intellectual capacity during mammalian evolution. The increased size of larger brains results primarily from a disproportionate expansion of the surface area of the layered sheet of neurons comprising the cerebral cortex (1–7), with the appearance of convolutions of the cortical surface (with crests known as gyri and intervening grooves called sulci) providing a means of increasing the total cortical area in a given skull volume. This horizontal expansion of the cerebral cortex is not accompanied by a comparable increase in cortical thickness; in fact, the 1000-fold increase in cortical surface area between human and mouse is only accompanied by an ~twofold increase in cortical thickness (8).

The cerebral cortex is organized into columnar functional units (9), and the expansion of the cerebral cortex appears to result from increases in the number of radial columns rather than from increases in individual column size (5, 10). These observations have

led to the proposal that increases in the number of columns result from a corresponding increased number of progenitor cells (5). It has been suggested that minor changes in the relative production of progenitors and neurons could produce dramatic increases in cortical surface area (5, 11).

One protein that might regulate the production of neural precursors is β -catenin, an integral component of adherens junctions (12) that interacts with proteins of the T cell factor/lymphoid enhancer binding factor (TCF/LEF) family to transduce Wnt signals (13). Wnts (a family of secreted signaling molecules that regulate cell growth and cell fate) (14) and TCF/LEF family members (15, 16) are expressed in overlapping patterns in the developing mammalian brain, and numerous studies support the role of Wnt signaling in cell fate regulation during development (17). Inactivation of specific Wnts (18, 19), TCF/LEF members (20), or β -catenin (21) results in specific developmental brain defects, and persistent activation of β -catenin has been implicated in a variety of human cancers (13), including some resembling neural precursors such as medulloblastoma (22). These findings raise the possibility that β -catenin influences cell number or cell fate decisions in the developing nervous system.

β -catenin is widely expressed in many tissues (23). To examine more closely the expression patterns of β -catenin during mammalian

¹Department of Pathology, Brigham and Women's Hospital, Boston, MA 02115, USA. ²Division of Neurogenetics, Department of Neurology, Beth Israel Deaconess Medical Center, Boston, MA 02115, USA.

*Present address: Department of Pathology, Northwestern University School of Medicine, 303 East Chicago Avenue, Chicago, IL 60611–3008, USA.

†To whom correspondence should be addressed. E-mail: cwalsch@caregroup.harvard.edu

RESEARCH ARTICLES

neural development, in situ hybridization of β -catenin was performed on embryonic mouse brain sections. Strong hybridization was observed for β -catenin in neuroepithelial precursors in the ventricular zone across the period during which neurons were produced (Fig. 1A). Immunostaining with a monoclonal antibody

indicates that, in neuroepithelial precursors, β -catenin protein is enriched at adherens junctions at the lumen of the ventricle, where it colocalizes in rings with F-actin, highlighted by rhodamine phalloidin (Fig. 1B).

To examine whether activating β -catenin signaling could regulate mammalian brain

development, we generated transgenic mice overexpressing an NH₂-terminally truncated form of β -catenin fused at the COOH-terminal with green fluorescent protein (GFP) (Δ N90 β -catenin-GFP) in neuroepithelial precursors. NH₂-terminally truncated β -catenin no longer requires Wnt signaling for sustaining activity, because it lacks key phosphorylation sites for GSK3 β that normally target it for destruction in the absence of Wnts (24). This form of β -catenin is stabilized constitutively in vivo and remains able to bind E-cadherin and α -catenin and to activate transcription by binding with TCF/LEF cofactors (24, 25) (Fig. 2B) [see supplementary online material (SOM)]. The expression of Δ N90 β -catenin-GFP was driven by the enhancer element contained in the second intron of the nestin gene (Fig. 2C) (see SOM), which directs expression in central nervous system progenitor cells (26).

Transgenic embryos at embryonic day 15.5 (E15.5) have grossly enlarged brains, with a considerable increase in the surface area of the cerebral cortex, without a corresponding increase in cortical thickness ($n = 10$) (Fig. 3). Sections through the forebrain revealed that, in transgenic brains, the horizontal growth of the tissue is so extensive that the normally smooth cerebral cortex of the mouse forms undulating folds resembling the gyri and sulci of higher mammals (Fig. 3B) (27). Brains from E17.5 embryos showed similar enlargement and folding (fig. S1). In

Fig. 1. Expression of β -catenin transcript and protein in neural precursors. **(A)** β -catenin in situ hybridization in sections through developing mouse cerebral cortex. β -catenin is strongly expressed in the ventricular zone (VZ) precursor cells at all ages during which cortical neurons are generated. A weaker signal is present in the developing cortical plate. Bar, 200 μ m. **(B)** Immunostaining through E14.5 mouse ventricular zone reveals β -catenin immunoreactivity (green) concentrated in rings at the luminal surface. Staining of the same section with rhodamine phalloidin reveals F-actin (red), which colocalizes with adherens junctions in a ringlike distribution at the luminal surface. The merged view indicates that β -catenin colocalizes with phalloidin. Bar, 10 μ m.

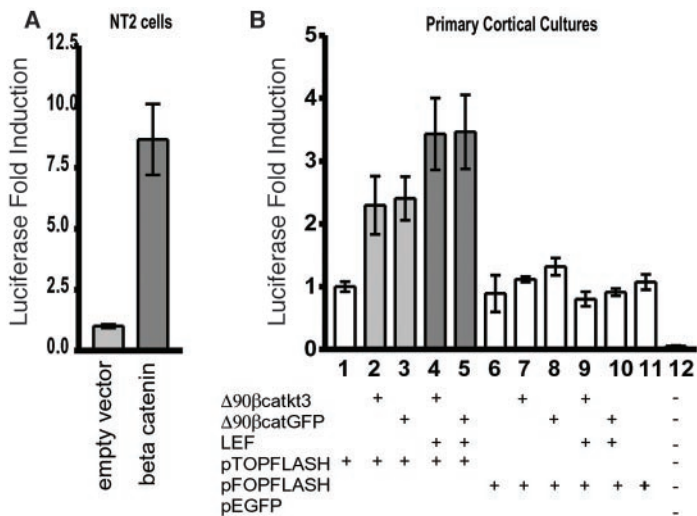
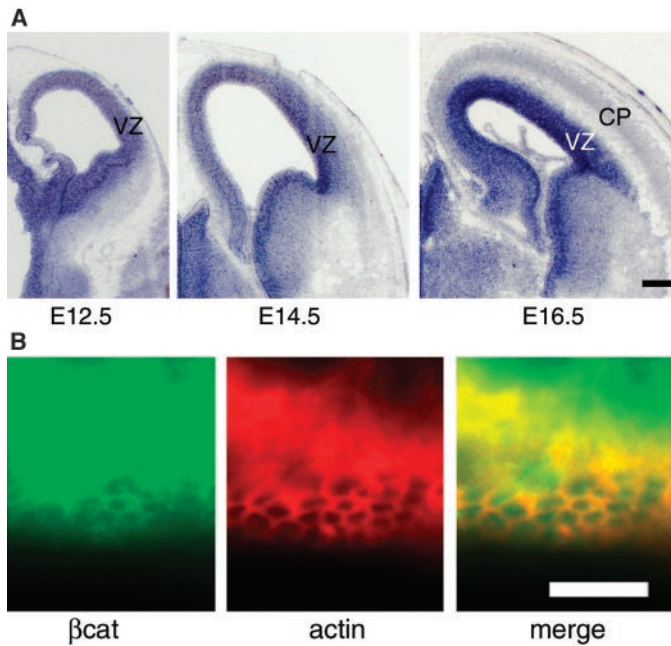


Fig. 2. Transcriptional activation by β -catenin and expression and transgenic construct design. **(A)** pTOPFLASH luciferase reporter assay in NT-2 cells. NT-2 cells were transfected with pTOPFLASH, containing four consensus LEF-1/TCF-1 binding sites, a minimal Fos promoter, and a luciferase reporter (43). Transfections were performed with and without cytomegalovirus (CMV)- Δ 90 β -catenin-GFP. CMV-LacZ was used to normalize for transfection efficiency. Twenty-four hours later, cells were lysed and protein extracts were assayed for luciferase. Fold inductions of luciferase activity represent the average of three experiments, with error bars representing one SEM. **(B)** Δ 90 β -catenin activates transcription in primary cortical cells. Primary cells from E17 cortex were transfected with the pTOPFLASH luciferase reporter

construct and the expression vectors as indicated. Luciferase activity was assayed 48 hours after transfection. Fold inductions represent the average of six experiments, with error bars indicating one SEM. **(C)** Expression and transgenic constructs. Constructs removing the NH₂-terminal 90 amino acids of mouse β -catenin are fused either to EGFP or the kt3 epitope tag. For expression in transient transcription assays, β -catenin constructs are placed behind the CMV promoter. The nestin second intron coupled with the thymidine kinase minimal promoter are used to generate transgenic mice. The first intron from the rat insulin II gene is incorporated to enhance expression levels. The same β -catenin alleles were used in both in vitro and transgenic mice.

resyl violet-stained sections, a densely stained layer of cells adjacent to the enlarged ventricular lumen morphologically resembled the proliferative zone of wild-type brains but was greatly expanded in surface area in the transgenic animals (E15.5, $n = 10$; E17.5, $n = 6$; E19.5, $n = 2$). Because we observed marked expansion of the cortical neuroepithelium, we focused our further studies on this population of cells at E15.5, an age midway through mouse cortical neurogenesis.

To determine the identity of the cells that may account for the expansion of the transgenic brains, we examined the expression of markers specific for neuroepithelial precursors and differentiating neurons. The basic helix-loop-helix transcription factors *Hes5*

and *Hes1* are downstream effectors of the Notch signaling pathway and regulate neuronal differentiation (28). *Hes5* is expressed specifically by neuroepithelial precursors, whereas *Hes1* is highly expressed in precursors, with lower expression in more differentiated cortical plate neurons (29). In situ hybridization for *Hes5* of comparable coronal sections through wild-type and transgenic brains suggests that the neural precursor population in transgenic animals is expanded (Fig. 4A). The expression of both *Hes1* (fig. S1) and *Ki67* (Fig. 5), a protein expressed in all dividing cells (30, 31), highlighted the ventricular zone and confirmed the findings seen with *Hes5*, providing further support that the precursor zone is expanded in trans-

genic animals. Finally, we used the thymidine analog BrdU to label dividing neural precursor cells by exposing embryos to BrdU for 30 min before killing them. Sections through wild-type and transgenic brains show that the same cells lining the ventricle also incorporate BrdU, confirming that the population of cells labeled with the precursor markers is composed of dividing cells (Fig. 3, E and F).

To investigate the spatial patterns of neuronal differentiation in transgenic animals, we examined the expression of three different markers of cortical neuron populations—Reelin (*Reln*), T-box brain gene 1 (*Tbr-1*), and TuJ1. In wild-type mice at E15.5, *Reln* labels Cajal-Retzius neurons in the outermost rind of cells of the developing cortical plate (Fig. 4). Similarly, in the brains of transgenic animals, in situ hybridization for *Reln* expression showed strong labeling in its normal position at the margin of the cortical plate. In wild-type mice at E15.5, *Tbr-1* is normally expressed in neurons of the cortical preplate and subplate (Fig. 4). Similarly, in situ hybridization for *Tbr-1* in transgenic animals indicates that cortical cells outside the ventricular zone expressed *Tbr-1* (Fig. 4). The general pattern of *Tbr-1* staining resembled that of wild-type animals, with *Tbr-1*-expressing cells situated in the region outside the progenitor zone in the developing cortical plate. However, much like those that express *Reln*, the cells that express *Tbr-1* were somewhat more widely scattered throughout the developing cortical plate, as compared with cells with wild-type expression. In E15.5 wild-type animals, TuJ1 labels newly differentiated neurons outside the ventricular zone (Fig. 4). In transgenic mice, TuJ1 immunoreactivity also labeled the layer of cells outside the ventricular zone, supporting the idea that postmitotic neurons remain localized outside the ventricular zone in transgenic animals. Despite the massive expansion of cortical surface area, transgenic precursors appear to differentiate into young neurons in an approximately normal spatial pattern. Taken together, these expression studies suggest that over-activating β -catenin does not disrupt the normal developmental sequence of neuronal differentiation, and the horizontal expansion of the cortical plate is a result of an increased number of proliferative precursor cells.

Enlargement of the precursor pool in transgenic brains can result from increased mitotic rates, decreased cell death, changes in cell fate choice (whether to differentiate or to proliferate), or any combination of these factors. To examine whether the horizontal expansion of the progenitor pool in transgenic animals results from increased mitotic rates, we counted the proportion of precursor cells that could be labeled by a 30-min pulse of BrdU. To quantify the fraction of cells in S phase, we obtained a labeling index (LI) by counting the percentage of cortical progenitor cells that were labeled by a single pulse of

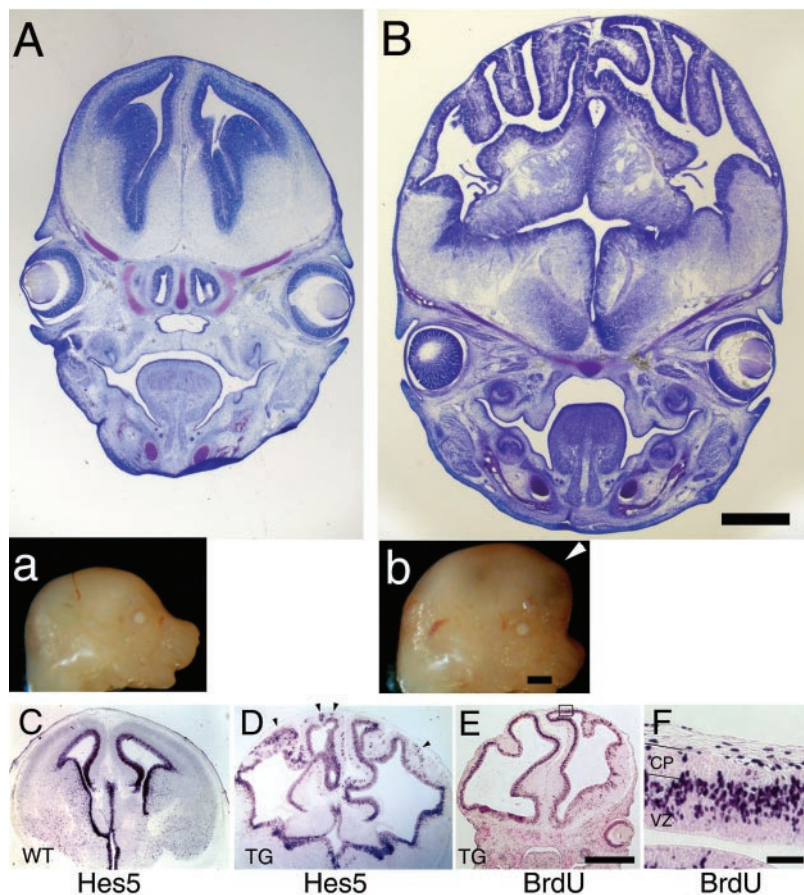


Fig. 3. Enlarged brains and heads of β -catenin transgenic animals with horizontal expansion of precursor population. Mid-coronal section through the forebrain stained with cresyl violet of an embryonic day 15.5 wild-type littermate control (A) and comparable section of a transgenic animal (B) expressing a $\Delta 90\beta$ -catenin-GFP fusion protein in neural precursors. The forebrain of transgenic animals is enlarged overall, with increased surface area and folding of the epithelial surface. Bar, 1 mm. Insets: Images of wild-type (a) and of transgenic (b) heads reveal gross enlargement of the skull and forebrain vesicles protruding anteriorly (as indicated by the white arrowhead) over the face of the embryo. Bar, 2 mm. (C and D) In situ hybridization for *Hes5* in comparable coronal sections through wild-type littermate control (C) and transgenic brain (D). *Hes5* is expressed in progenitor cells in the ventricular zone of wild-type and transgenic brains. Additional areas of *Hes5*-expressing cells are located in ectopic regions away from the ventricular lumen in transgenic animals (as indicated by the black arrowheads). Bar, 1 mm. (E and F) BrdU-labeled cells in transgenic animals after a 30-min exposure to BrdU. BrdU labels the same cells as the progenitor markers *Hes5* and *Hes1*. (F) Higher magnification image reveals that the overall organization of the ventricular zone of transgenic animals is preserved, with S-phase progenitors occupying the outer half of the ventricular zone, similar to wild-type progenitors. Bar, 1 mm (E), 200 μ m (F).

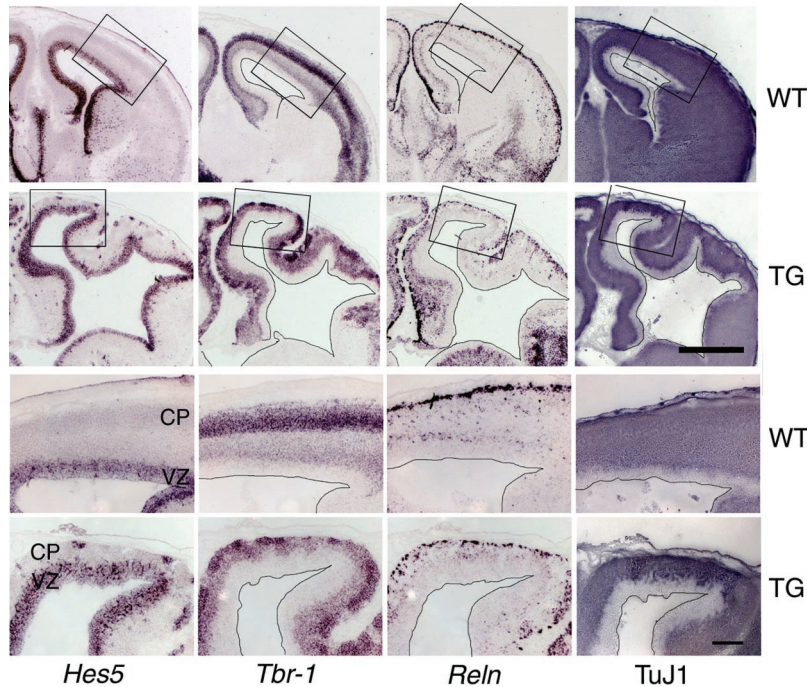


Fig. 4. Neuronal differentiation in transgenic brains. In situ hybridization for *Hes5* labels cortical precursors (adjacent to lumen of ventricle), but not differentiated neurons in both E15.5 wild-type and transgenic brains. In situ hybridization for *Tbr-1* in adjacent sections indicate that *Tbr-1* is expressed in the cortical plate and intermediate zone, but not in the precursor zone of both control and transgenic brains. In situ hybridization of adjacent sections show strong *Reln* expression in the outermost layer of neurons of both control and transgenic brains. Sections stained with the TuJ1 antibody reveal the location of newly postmitotic neurons in the intermediate zone and developing cortical plate, but not in the ventricular zone in both wild-type and transgenic animals. The relative position of *Hes-5*, *Tbr-1*, *Reln*, and TuJ1 staining is maintained in wild-type versus transgenic animals. The boxed portion in the upper panels is enlarged in the lower panels. The ventricular surface is outlined to aid visualization. Bar, 1mm (top) and 200 μ m (bottom).

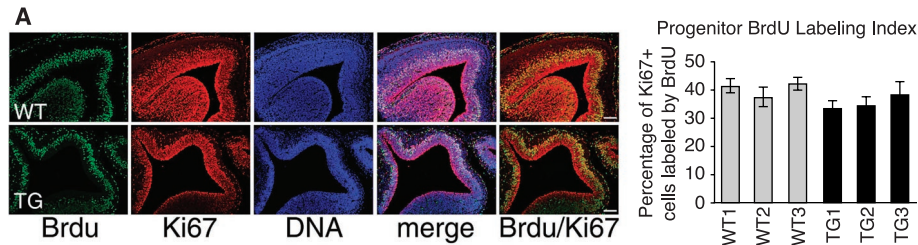


Fig. 5. Cell cycle re-entry increased in transgenic precursors. (A) The percentage of progenitor cells (Ki67+, red) labeled with BrdU (green) after a 30-min pulse label is not altered in transgenic animals. DNA stain (blue) reveals that wild type developing cortex is thicker outside the progenitor population, containing relatively more postmitotic cells (Ki67-), as compared with transgenic brains [$F_{(6,18)} = 0.970$, $P = 0.471$]. (B) Normalized for area, transgenic brains have more apoptotic cells labeled by TUNEL (red). DNA is counterstained (blue) with Hoechst 33342 [$F_{(4,11)} = 26.00$, $P = 0.0002$]. (C) Animals were exposed to a single-pulse label of BrdU 24 hours before being killed; sections were stained with antibodies to BrdU (green) and Ki67 (red). The fraction of cells labeled only with BrdU (BrdU+/Ki67-, no longer dividing) 24 hours after pulse label, as compared with BrdU+/Ki67+ cells (yellow, re-entered cell cycle). Approximately twice as many wild-type precursors leave the cell cycle, as compared with transgenic precursors [$F_{(4,15)} = 11.00$, $P = 0.0009$].

BrdU. Progenitor cells were identified by Ki67 immunoreactivity (30, 31). Because in mammalian cells the length of S phase remains relatively constant while the length of G_1 regulates proliferation (32), this LI provides an estimation of cell cycle length. If the cell cycle is shortened, the relative fraction of cells labeled by a brief BrdU pulse will increase. Examination of random fields chosen from six brains (three wild-type and three transgenic brains) suggests that the transgenic neural precursors did not divide significantly faster than did normal wild-type precursors [$F_{(6,18)} = 0.970$, $P = 0.471$] (Fig. 5A).

Programmed cell death (apoptosis) occurs during normal development of the central nervous system (33), and decreased programmed cell death may be one mechanism underlying the increased brain size of transgenic animals. Apoptotic cell death was examined using TUNEL staining in wild-type and transgenic brains. TUNEL+ cells were confirmed by verifying condensed nuclei labeled with the DNA binding dye Hoechst 33342. Counts of total numbers of labeled cells revealed that cell death in transgenic brains was not substantially less than found in wild type (Fig. 5B); in fact, there appeared to be greater than twofold increased rates of apoptosis in transgenic brains [$F_{(4,11)} = 26.00$, $P = 0.0002$]. Taken together, the BrdU-labeling studies and TUNEL studies suggest that the progenitor cell population expansion cannot be explained by a simple mitogenic effect of β -catenin or by decreased apoptotic cell death.

Progenitor divisions that give rise to additional progenitors can expand the progenitor pool exponentially. Consequently, small alterations in the fraction of cell divisions that expand the progenitor pool can result in large changes in the final size of the brain (5, 34). To examine whether the increase in the progenitor pool results from a shift in the fraction of progenitors that choose to remain progenitors instead of differentiating, we examined cell cycle exit and re-entry by examining the fraction of cells dividing after pulse labeling with BrdU 24 hours earlier. We identified cells that had left the cell cycle as BrdU+ and Ki67-, and we identified cells that remained in the cell cycle as BrdU+ and Ki67+. At E15.5, we found an ~twofold increase in the proportion of transgenic precursors that re-enter the cell cycle when compared with wild-type neural precursors [$F_{(4,15)} = 11.00$, $P = 0.0009$] (Fig. 5C). Together, these studies suggest that β -catenin activation functions in neural precursors to influence the decision to re-enter the cell cycle instead of differentiate.

Our results support recent findings suggesting that epithelial architecture and adherens junctions regulate growth control and cell proliferation (35). Because β -catenin is an integral component of adherens junctions (12), disruptions of adherens junctions may cause misregu-

lation and accumulation of cytoplasmic β -catenin. Our findings that β -catenin signaling can regulate the decisions of neural precursors to re-enter or exit the cell cycle lend support to the possibility that β -catenin signaling may mediate the loss of growth control when adherens junctions are disrupted.

It has been hypothesized that mutations in regulatory genes that control the decision of neural precursors to divide or differentiate can underlie the expansion of the precursor population without changing the thickness of the cortex (5, 11). Here, we find that β -catenin activation can regulate the size of the neural precursor pool by influencing the decision to divide or differentiate, without increasing cell cycle rate, decreasing cell death, or grossly altering neuronal differentiation. Larger brains can be generated in different ways as well. For example, reduction of programmed cell death by targeted mutation of Caspase 9 causes severe brain malformations characterized by cerebral enlargement, ectopic growth, and thickening of the ventricular zone (36, 37). In contrast, mice with targeted deletions of the cell cycle regulator $p27^{kip1}$ have increased body size and uniformly enlarged brains with virtually no anatomic abnormalities other than increased cell number and cell density (38–40). Notably, cortical surface area was not disproportionately increased (38). In contrast, our findings suggest that subtle changes in the expansion or maintenance of the neural precursor population result in horizontal expansion of the surface area of the developing cerebral cortex without increases in cortical thickness (41). Further understanding of how the decision to divide or differentiate is regulated by β -catenin will lend valuable insight into the mechanisms that underlie the disproportionate growth of the cerebral cortex in higher mammals.

References and Notes

1. B. L. Finlay, R. B. Darlington, *Science* **268**, 1578 (1995).
2. R. A. Barton, P. H. Harvey, *Nature* **405**, 1055 (2000).
3. D. A. Clark, P. P. Mitra, S. S. Wang, *Nature* **411**, 189 (2001).
4. V. S. Caviness Jr., T. Takahashi, R. S. Nowakowski, *Trends Neurosci.* **18**, 379 (1995).
5. P. Rakic, *Trends Neurosci.* **18**, 383 (1995).
6. H. Elias, D. Schwartz, *Science* **166**, 111 (1969).
7. H. Haug, *Am. J. Anat.* **180**, 126 (1987).
8. P. Rakic, *Science* **241**, 170 (1988).
9. V. B. Mountcastle, *Brain* **120**, 701 (1997).
10. Although the pyramidal neurons comprising the majority of cerebral cortical neurons appear to be generated in an approximately columnar arrangement, not all cortical neurons are derived from cortical ventricular zone progenitors, because the majority of cortical inhibitory interneurons are generated outside the cerebral cortex (42).
11. V. J. Caviness, T. Takahashi, R. S. Nowakowski, *Trends Neurosci.* **18**, 379 (1995).
12. R. T. Cox, C. Kirkpatrick, M. Leifer, *J. Cell Biol.* **134**, 133 (1996).
13. M. Peifer, P. Polakis, *Science* **287**, 1606 (2000).
14. B. A. Parr, M. J. Shea, G. Vassileva, A. P. McMahon, *Development* **119**, 247 (1993).
15. M. Oosterwegel et al., *Development* **118**, 439 (1993).
16. E. A. Cho, G. R. Dressler, *Mech. Dev.* **77**, 9 (1998).
17. R. T. Moon, J. D. Brown, M. Torres, *Trends Genet.* **13**, 157 (1997).
18. A. P. McMahon, A. Bradley, *Cell* **62**, 1073 (1990).
19. S. M. Lee, S. Tole, E. Grove, A. P. McMahon, *Development* **127**, 457 (2000).
20. J. Galceran, E. M. Miyashita-Lin, E. Devaney, J. L. Rubenstein, R. Grosschedl, *Development* **127**, 469 (2000).
21. V. Brault et al., *Development* **128**, 1253 (2001).
22. H. Huang et al., *Am. J. Pathol.* **156**, 433 (2000).
23. S. Butz, L. Larue, *Cell Adhes. Commun.* **3**, 337 (1995).
24. H. Clevers, M. van de Wetering, *Trends Genet.* **13**, 485 (1997).
25. A. I. Barth, A. L. Pollack, Y. Altschuler, K. E. Mostov, W. J. Nelson, *J. Cell Biol.* **136**, 693 (1997).
26. P. J. Yaworsky, C. Kappen, *Dev. Biol.* **205**, 309 (1999).
27. Although the gyral convolutions of the adult human cortex also span all cortical layers, the ventricular surfaces remain relatively smooth, contrasting with the convoluted ventricular surfaces of β -catenin-transgenic animals. Despite this difference, sections through developing human brains show that the neural progenitor population in humans, like that of β -catenin-transgenic animals, consists of a thin, horizontally expansive epithelial sheet. Relative differences in the degree of mismatch between cortical surface area to skull volume may determine when cortical folding occurs and whether the resulting folding affects the entire cortical thickness.
28. T. Ohtsuka, M. Sakamoto, F. Guillemot, R. Kageyama, *J. Biol. Chem.* **276**, 30467 (2001).
29. T. Ohtsuka et al., *Embo J.* **18**, 2196 (1999).
30. T. Scholzen, J. Gerdes, *J. Cell Physiol.* **182**, 311 (2000).
31. N. Kee, S. Sivalingam, R. Boonstra, J. M. Wojtowicz, *J. Neurosci. Methods* **115**, 97 (2002).
32. C. V. DiSalvo, D. Zhang, J. W. Jacobberger, *Cell Prolif.* **28**, 511 (1995).
33. C. Y. Kuan, K. A. Roth, R. A. Flavell, P. Rakic, *Trends Neurosci.* **23**, 291 (2000).
34. T. Takahashi, R. S. Nowakowski, V. S. Caviness Jr., *J. Neurosci.* **16**, 6183 (1996).
35. D. Bilder, M. Li, N. Perrimon, *Science* **289**, 113 (2000).
36. K. Kuida et al., *Cell* **94**, 325 (1998).
37. R. Hakem et al., *Cell* **94**, 339 (1998).
38. M. L. Fero et al., *Cell* **85**, 733 (1996).
39. H. Kiyokawa et al., *Cell* **85**, 721 (1996).
40. K. Nakayama et al., *Cell* **85**, 707 (1996).
41. For a discussion of potential mechanical forces that lead to cortical folds, see D. C. Van Essen, *Nature* **385**, 313 (1997).
42. S. A. Anderson, O. Marin, C. Horn, K. Jennings, J. L. Rubenstein, *Development* **128**, 353 (2001).
43. M. van de Wetering et al., *Cell* **88**, 789 (1997).
44. Supported by National Institute of Neurological Disorders and Stroke grant R01NS32457 (C.W.). A. C. was a Howard Hughes Medical Institute Physician Postdoctoral Fellow. We thank A. Barth and W. J. Nelson, Stanford, for $\Delta N90\beta$ -catenin-kt3 DNA reagent; J. M. Hebert, A. Okada, and S. K. McConnell, Stanford, for nestin, enhanced green fluorescent protein (EGFP) constructs; M. van de Wetering, Utrecht, for pTOPFLASH and pPOFLASH reagent; E. Fuchs, University of Chicago, for hLef1 reagent; R. Kageyama for *Hes1* and *Hes5* in situ probes; R. R. Ratan, Harvard, for the luminometer; U. Berger for in situ; L. Du, T. Thompson, and S. White for technical assistance; P. Webster, Zymogenetics, for transgenic construct design; and X. He and members of the Walsh lab for comments on the manuscript.

Supporting Online Material

www.sciencemag.org/cgi/content/full/297/5580/365/DC1

Materials and Methods

References and Notes

Fig. S1

21 May 2002; accepted 25 June 2002

REPORTS

Nonresonant Multiple Spin Echoes

Thilo M. Brill,* Seungoh Ryu, Richard Gaylor, Jacques Jundt, Douglas D. Griffin, Yi-Qiao Song, Pabitra N. Sen, Martin D. Hürlimann

Nonresonant manipulation of nuclear spins can probe large volumes of sample situated in inhomogeneous fields outside a magnet, a geometry suitable for mobile sensors for the inspection of roads, buildings, and geological formations. However, the interference by Earth's magnetic field causes rapid decay of the signal within a few milliseconds for protons and is detrimental to this method. Here we describe a technique to suppress the effects of Earth's field by using adiabatic rotations and sudden switching of the applied fields. We observed hundreds of spin echo signals lasting for more than 600 milliseconds and accurately measured the relaxation times of a liquid sample.

Conventional nuclear magnetic resonance (NMR) experiments are almost always carried out by manipulating nuclear spins using

radio frequency (rf) pulses at the spin Larmor frequency $\omega = \gamma B$, where γ is the gyromagnetic ratio and B is the magnitude of the

magnetic field. Such resonant NMR experiments allow the imaging of spins in materials and the characterization of spin interactions, enabling applications extending to materials such as soft condensed matter (1), plants (2), food products (3), cement and concrete (4), and geological materials (5, 6). The field applications are the motivation for several recent developments in ex situ NMR (7–10), where a mobile NMR detector is used to examine the sample outside the NMR magnet. However, as a result of the geometry of such mobile tools, the applied magnetic fields exhibit large inhomogeneities, and all resonant techniques will result in small sensitive volumes where the resonance condition is satisfied. Composite (11) and adiabatic (12) pulses may be used to expand the excitation bandwidth to a limited extent at the expense of higher irradiation power.

Alternatively, spins can be manipulated